Journal of Applied Pharmaceutical Science Vol. 13(10), pp 119-131, October, 2023
Available online at http://www.japsonline.com
DOI: 10.7324/JAPS.2023.116845
ISSN 2231-3354

Chemo-profiling and bioactivities of Taif rose (*Rosa damascena* Mill.) industrial by-products after hydrodistillation

Ezzat E. A. Osman[1*], Salih A. Bazaid[2], El-Sayed S. Abdel-Hameed[1]

[1]Department of Medicinal Chemistry, Theodor Bilharz Research Institute, Giza, Egypt.
[2]College of Sciences, Taif University, Taif, Saudi Arabia.

ARTICLE INFO

Received on: 19/05/2023
Accepted on: 06/09/2023
Available Online: 04/10/2023

Key words:
Anticancer, antioxidant, industrial wastes, phytochemicals, *R. damascena.*

ABSTRACT

This study investigated the chemical composition of *Rosa damascena* Mill. (grown in the Taif region of Saudi Arabia), in relation to their potential as antioxidants and anticancer agents. The rose flowers are used to produce essential oils and hydrosol, but the process generates a significant amount of —solid and liquid. They contain biologically active compounds and can be treated as by-products. This study aimed to characterize these materials and analyze their extracts for biological activity. The total phenolic, flavonol, and flavonoid contents were quantified, and their chemical compositions were determined using liquid chromatography-mass spectrometry analysis. The antioxidant properties were estimated *in vitro* using three methods [1,1-diphenyl picrylhydrazyl (DPPH) radical, phosphomolybdenum, and ferric reducing power assays], while an anticancer test was carried out using the liver carcinoma cell line (HepG2). The findings showed that the texture's *n*-butanol (*n*-BuOH) fraction had the highest overall phenolic, flavonoid, and flavonol contents (230.69 ± 10.50 mg gallic acid equivalents /g ext., 71.66 ± 3.15 mg RE/g ext., and 51.70 ± 0.61 mg QE/g ext., respectively). The liquid chromatography-electrospray ionization-mass spectrometry analysis of the by-product extracts led to identifying 55 polyphenolic compounds, including organic acids, flavonoids, phenolic acids, and tannins, of which some constituents were described in *Rosa* extracts for the first time. In addition, the *n*-BuOH fraction of the texture and wastewater had a significant DPPH radical scavenging activity with SC_{50s} values of 7.57 ± 0.01 and 12.78 ± 0.13 µg/ml, respectively. Furthermore, the cytotoxic activity of the *n*-BuOH fraction of texture showed the highest activity on HepG2 (IC_{50} = 12.1 ± 0.85 µg/ml) followed by wastewater *n*-BuOH fr. (IC_{50} = 14.00 ± 1.05 µg/ml) and the methanolic extract of texture (IC_{50} = 20.5 ± 1.41 µg/ml). Our findings indicated that rose industrial by-products are enriched with polyphenolic compounds with promising antioxidants and anticancer activities. Thus, they could be used as a food supplement.

INTRODUCTION

The Taif region in Saudi Arabia is famous for the cultivation of a kind of Damask rose known as *Rosa damascena* Mill. *var. trigintipetala* Dieck or Taif rose. The plant is considered an important economical source of essential oil and floral water (Dobreva *et al*., 2020). Furthermore, local rose oil is recognized as one of the most distinguished and reputational perfumes around the globe (Abdel-Hameed *et al*., 2016). After the production of essential oil with hydrodistillation technology, a huge amount of waste materials (by-products), including texture and wastewater, is produced. They are usually discarded as industrial waste without effective use and cause environmental pollution (Gerasimova *et al*., 2022). However, the by-products can also be used in the production of methane biogas, phenyl ethyl alcohol, compost, residue concrete, health sludge, cosmetics, and natural antioxidant supplement (Erbaş and Baydar, 2016). Bulgarian and Greece *R. damascena* wastewater extracts after oil production are rich in polyphenols, which hardly degrade and have remarkable bioactivities (Ilieva *et al*., 2022). Other studies reported the existence of various secondary metabolites, including quercetin, kaempferol, ellagic acid, and their glycoside derivatives, as well as observing some pharmacological properties (Dina *et al*., 2021; Kumar *et al*., 2008; Rusanov *et al*., 2014; Schiber *et al*., 2006; Sabahi *et al*., 2020). Our previous studies were focused on the chemical profiling of the nonpolar constituents of

**Corresponding Author*
Ezzat E. A. Osman, Department of Medicinal Chemistry, Theodor Bilharz Research Institute, Giza, Egypt. E-mail: ezzat_ea @ yahoo.com

R. damascena and the evaluation of their cytogenetic and cytotoxic activities in which both absolute rose oil and concrete were safe at a concentration of 10 µg/ml on normal human blood lymphocytes. Moreover, the concrete exerted cytotoxic activity against HepG2 and MCF7 cell lines with IC_{50} = 16.28 and 18.09 µg/ml, and the absolute oil had IC_{50} of 24.94 and 19.69 µg/ml, respectively. The nonpolar constituents were investigated using gas chromatography-mass spectrometry, which led to the phenyl ethanol, β-citronellol, geraniol, eugenol, and methyl eugenol being the major constituents (Hagag *et al*., 2014). On the other hand, the liquid chromatography-electrospray ionization-mass spectrometry (LC-ESI-MS) was used to characterize the polar constituents, and the results revealed the existence of 28 compounds categorized as phenolic acids, ellagitannins, and flavonoids (Abdel-Hameed *et al*., 2013). To the best of our knowledge, an excellent safety effect of *R. damascena* wastewater extracts on chronic, subchronic, and acute toxicity in adult albino mice was observed. In addition, the total phenolic, flavonoid, and flavonol contents as well as their antioxidant potentials have been estimated (Abdel-Hameed *et al*., 2015).

Hepatic cells are important in the drug development process because the liver is the major detoxification organ of the human body and is primarily involved in drug metabolism and interactions. Hence, HepG2 cells are the most commonly used *in vitro* models, particularly in the study of liver physiology and cancer (Harjumäki *et al*., 2019).

Herein, the industrial by-products (wastewater and texture) after the hydrodistillation method were phytochemically investigated by determining their phenolic, flavonol, and flavonoid contents. Afterward, the polar active ingredients were characterized using LC-ESI-MS analysis. Furthermore, the anticancer effects using HepG2 cells of *Rosa* by-product extracts and the antioxidant potentials were evaluated.

MATERIALS AND METHODS

Chemicals

The reagents 1,1-diphenyl picrylhydrazyl (DPPH$^{\bullet}$) free radical, Folin–Ciocalteu's reagent (FCR), sodium carbonate, sodium phosphate, aluminum chloride ($AlCl_3$), ammonium molybdate, ascorbic acid, sulphorhodamine-B (SRB), the acids, and all organic solvents were of analytical grade and purchased from Sigma-Aldrich Chemicals, USA.

Collection of plant materials

Rosa damascena flowers were collected during the harvest season (March-April) from the Taif region for the production of essential oil. A fresh sample of the plant was verified by Prof. Mohamed Fadle, Professor of Plant Taxonomy, Faculty of Science, Taif University, KSA. A voucher sample (no. 1532018) was preserved at the Department of Medicinal Chemistry, Theodor Bilharz Research Institute, Giza, Egypt. In rose oil production factories, the freshly collected flowers were mixed with water in a tin-lined copper boiler (10,000 roses × 50 l water), then simmered gently by the gas heater for about 6–10 hours according to the boiler size. After the essential oil production, a huge amount of by-products (wastewater and texture) was collected in the distillation container.

Preparation of extracts

Four liters of *R. damascena* industrial by-products were collected from one of Taif's rose oil factories, then filtrated by cleaned cotton bags by squeezing the texture separated from the wastewater. Three hundred grams of texture by-product was extracted by methanol (MeOH) for one week at room temperature. A rotary evaporator (Buchi, Switzerland) was used to remove the solvent under pressure to afford 74.63 g of MeOH extract from the texture (MT); this step was repeated two times. In parallel, the wastewater obtained from squeezing the original by-product was centrifuged and filtered by Whatman No. 1 filter paper, then the filtrate was evaporated to yield 54.31 g of dried wastewater extract (W). Moreover, 20 g of each of the MT and W extracts were dissolved in 120 ml of distilled water, then partitioned with *n*-BuOH (3 × 120 ml). The organic and aqueous layers were separated and dried to give 7.62 g of *n*-BuOH fr. from texture MeOH extract (BT), 11.80 g of aqueous fraction from texture MeOH extract (AT), 5.71 g *n*-BuOH fraction from wastewater extract (BW), and 13.82 g aqueous fraction from wastewater extract (AW), respectively, as shown in Figure 1. All extracts were stored in brown glass bottles at room temperature for biological and chemical studies.

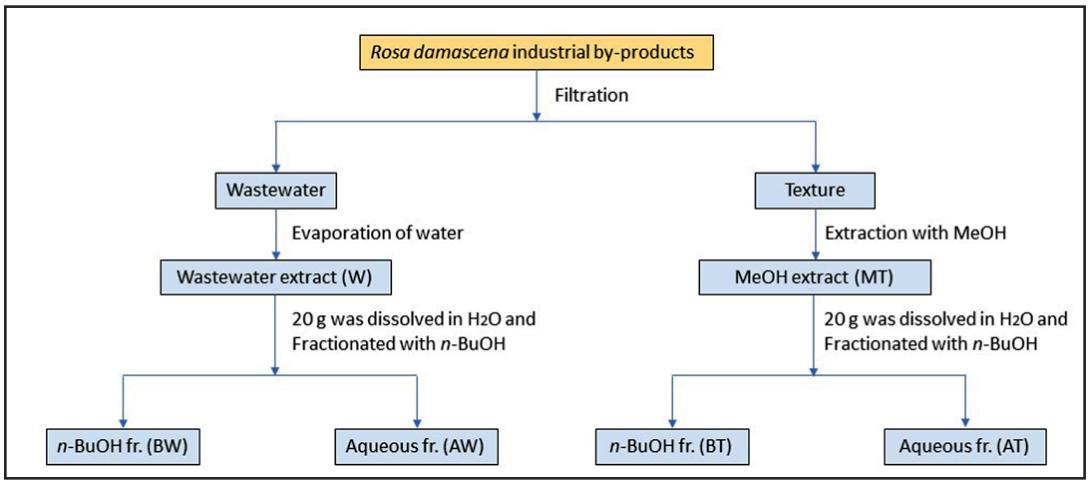

Figure 1. A scheme of extraction and fractionation process of *R. damascena* industrial by-products.

Phytochemical analysis

Quantification of total phenolic content

FCR assay was used to determine the total phenolic content tested extracts as described previously by Abdel-Hameed *et al*. (2009). Briefly, the tested extracts (100 µl) at a concentration of 100 µg/ml were mixed with FCR (500 µl) and neutralized with 20% Na_2CO_3 solution (1.5 ml). The reaction mixture was carefully stirred, diluted with distilled water to a volume of 10 ml, and incubated for 2 hours at room temperature to allow for color development. At 765 nm, the absorbance was recorded in comparison to a blank that had all the reagents without samples at the same conditions using a UV-visible spectrophotometer (Jenway 6405, USA). The total phenolic content was measured using gallic acid as a reference and expressed as milligram gallic acid equivalents (GAE) per gram of extract.

Quantification of total flavonoid content

The flavonoid content was analyzed by the $AlCl_3$ colorimetric method (Abdel-Hameed *et al*., 2009). Briefly, each extract (100 µl) at a concentration of 100 mg/ml was added to 2% $AlCl_3$ (100 µl) dissolved in ethanol, acetic acid one drop, and the mixture was diluted up to 5 ml. After 40 minutes at ambient temperature, the reaction mixture's absorbance was measured at 415 nm against a blank containing all reagents without the samples using a UV-visible spectrophotometer (Jenway 6405, USA). All determinations were carried out in triplicate, and rutin was used as a reference. The total phenolic content was calculated as milligram rutin equivalents (REs) per gram of extract.

Quantification of total flavonol content

The content of flavonols was examined using an $AlCl_3$ assay (Abdel-Hameed *et al*., 2009). Briefly, 1 ml of each sample solution (100 mg/ml) was mixed with 1 ml of $AlCl_3$ (20 mg/ml) and 3 ml of sodium acetate (50 mg/ml). The reaction mixture was shaken well, and the absorbance was recorded at 440 nm after 2.5 hours. Quercetin was used as standard, and the absorption of a quercetin solution in MeOH (0.5 mg/ml) was determined. The experiments were performed in triplicate, and the amount of total flavonols was measured in milligram of quercetin equivalents (QEs) per gram of extract.

LC-ESI-MS analysis

A hybrid 3100 mass detector system (Waters, Alliance, USA) was conducted in the high performance liquid chromatography system (2695-series) and coupled with an electrospray ionization (ESI) source. A membrane disc filter with a 0.45 m pore size was used to filter the mobile phases, then sonicated to remove any gases. After several optimization attempts, two mobile phases were used: mobile phase **A** consisted of distilled water acidified with 0.1% formic acid (FA), and mobile phase **B** consisted of acetonitrile/MeOH [1:1 v/v] acidified with 0.1% FA. Gradient elution was applied, using 5% B for 5 minutes, 10% B for 5 minutes, 50% B for 45 minutes, 95% B for 10 minutes, and finally 5% B for 5 minutes. The injection volume of the sample was 10 µl and the mobile phase flow rate (0.6 ml/minute) split 1/1 before the mass interface. With the following settings, the analysis was carried out in negative ion mode within the *m/z* 50–1,000 range and other parameters, including capillary voltage (3 kV), cone voltage (50 eV), ion source temperature (150°C), desolvation temperature (350°C), and cone gas flow (50 l/hours), and desolvation gas flow (600 l/hour). Polyphenols were identified based on their mass spectrum and retention time (tR) and information from the literature after the obtained MS data were processed using Maslynx 4.1 software.

Determination of the antioxidant activity

1, 1-Diphenyl-2-picrylhydrazyl radical assay

This technique relies on reducing the DPPH radical (purple color) to a diphenyl-picrylhydrazine stable molecule (yellow color). The DPPH radical scavenging activity was described by Osman *et al*. (2022). Briefly, 2 ml of *R. damascena* by-product extracts at different concentrations dissolved in MeOH was mixed with a 2 ml solution of 0.1 mM DPPH radical (dissolved in MeOH). The control contained 2 ml MeOH and 2 ml DPPH radical. The mixture was left to stand for 20 minutes at 37°C in the dark and a UV/Vis spectrophotometer (Jenway 6405, USA) was used to determine the absorbance at 517 nm. The experiment was performed in triplicate and ascorbic acid was used as a positive reference. The following equation was used to determine the DPPH radical scavenging rate:

$$\% \text{ DPPH radical scavenging activity} = [(A_C - A_S)/A_C] \times 100,$$

where A_S and A_C are the absorbances of the sample and control, respectively. The half-maximal scavenging concentration (SC_{50}) values were determined and expressed as the mean ± standard deviation (SD) in µg/ml.

Phosphomolybdenum assay

The phosphomolybdenum assay was carried out by the method of Prieto *et al*. (1999). It is predicated on the antioxidants' reduction of Mo (VI) to Mo (V) and the following formation of a green phosphate/Mo (V) complex. Briefly, 3 ml of the phosphomolybdenum reagent (28 mM sodium phosphate, 0.6 M sulfuric acid, and 4 mM ammonium molybdate) was added to 300 µl of the extract solution (100 µg/ml) in sealed test tubes. In a water bath set at 95°C, the reaction mixture was incubated for 90 minutes. The absorbance of the examined by-product extracts was measured at 695 nm using a UV/Vis spectrophotometer (Jenway 6405, USA) after cooling to room temperature in comparison with a blank sample containing 0.3 ml pure MeOH without extract. The experiment was performed in triplicate and the results were given in terms of milligram of ascorbic acid equivalents per gram of dried extracts (mg AAE/ g ext.).

Ferric reducing power (FRP) assay

This method was described by Abdel-Hameed *et al*. (2015). In total, 2 ml of by-product extracts (200 µg/ml) dissolved in MeOH was added to 2 ml of sodium phosphate buffer (0.2M, pH 6.6) and 2 ml of potassium ferricyanide (1%). The mixture was heated to 50°C in a water bath for 20 minutes. The mixture was then centrifuged at 3,000 rpm for 10 minutes at room temperature, with 2 ml of trichloroacetic acid (TCA) added. Immediately, 2 ml of the residual solution was added to 0.5 ml of 0.1% ferric chloride and 2 ml of MeOH. The absorbance of the samples, the blank, and the ascorbic acid reference were recorded at 700 nm using a

UV/Vis spectrophotometer (Jenway 6405, USA). All experiments were done in triplicate and ascorbic acid equivalents in milligram/gram of extract represented the FRP activity.

Determination of the anticancer activity

This assay was performed at the National Cancer Institute (NCI) in Egypt. *Rosa damascena* by-product extracts were tested *in vitro* using a HepG2 cell line (Obtained frozen in liquid nitrogen at −180°C from the American Type Culture Collection and were handled in NCI, by serial subculturing). Using SRB dye to stain the total amount of cellular protein, this assay indirectly calculates the number of cells. The test was described by Skehan *et al*. (1990). Briefly, at a concentration of 5×10^4–10^5 cells/well in a medium, the cells were seeded in 96-well microtiter plates and allowed to attach to the plates for 24 hours. Each individual sample was made in wells, which were then incubated for 48 hours at 37°C in 5% CO_2. After 24 hours, cells were treated with the relevant samples at different concentrations (0, 5, 12.5, 25, and 50 mg/ml). Then, the volume per well was increased to 200 ml using a fresh medium, and the incubation time was extended for another 24, 48, and 72 hours. After that, the cells were fixed with 50 µl of cold TCA (50%) for 1 hour at 4°C. Following the 30 minutes incubation, the cells were washed four times with 1% acetic acid. The plates were then desiccated and 100 µl/well of 10 mM Tris base (pH 10.5) was used to solubilize the dye for 5 minutes at 1,600 rpm on a shaker (Orbital shaker OS 20, Boeco, Germany). Using a spectrophotometer at 564 nm with an ELIZA microplate reader (Meter tech. Σ 960, USA), the optical density (OD) of each well was calculated.

The mean values of each drug concentration were computed after the mean background absorbances were automatically removed. For each cell line, the experiment was carried out three times. The following equation was used to determine the percentage of cell survival fraction:

$$\text{Survival fraction (\%)} = (OD_{\text{treated cells}} / OD_{\text{control cells}}) \times 100.$$

Statistical analysis

All determinations were carried out in triplicate and presented as mean ± SD using SPSS 13.0 program. The differences between each group were analyzed by one-way analysis of variance (ANOVA) with Tukey's *posthoc* test. Statistical significance was set to $p < 0.05$.

RESULTS AND DISCUSSION

Total phenolic, flavonoid, and flavonol contents

The waste materials of *R. damascena* were examined for their total phenolic, flavonoid, and flavonol contents. According to the findings shown in Table 1, the BT fraction represented the highest total phenolic, flavonoid, and flavonol contents (230.69 ± 10.50 mg GAE/g ext., 71.66 ± 3.15 mg RE/g ext., and 51.70 ± 0.61 mg QE/g ext., respectively) followed by the BW fraction (118.29 ± 2.92 mg GAE/g ext., 40.16 ± 1.05 mg RE/g ext., and 24.61 ± 0.75 mg QE/g ext., respectively). The MT extract (92.13 ± 4.18 mg GAE/g ext., 28.42 ± 0.63 mg RE/g ext., and 18.16 ± 0.81 mg QE/g ext., respectively) and the W extract (48.27 ± 1.27 mg GAE/g ext., 16.68 ± 0.73 mg RE/g ext., and 8.47 ± 0.44 mg QE/g ext.), respectively, had reduced amounts of the phenolic, flavonoid, and flavonol contents. The AW and AT fractions contained the lowest amounts. In comparison to published data, these results are in agreement with those of Baydar and Baydar (2013), who reported high phenolic content of Turkish *R. damascena* MeOH extract from spent flowers. Dina *et al*. (2021) reported the high phenolic and flavonoid contents of the aqueous extract of hydro-distilled petals of *R. damascena* growing in Greece. In contrast, other studies reported that the total phenolic and flavonoid contents in the wastewater of *R. damascene* were 7.2 ± 0.2 mg GAE/ml and 1.14 ± 0.01 mg/ml, respectively (Gateva *et al*., 2022). Thus, these results revealed that the geographical origin, extraction conditions, and solvent have significant effects on phenolic and flavonoid contents.

LC-ESI-MS analysis

The liquid chromatography coupled with mass spectrometer experiments were performed in order to investigate the phytoconstituents of *R. damascena* extracts. In total, 55 polyphenolic compounds, including organic acids, phenolic acids, tannins, and flavonoids, have been detected in the MT, W extracts, and their

Table 1. Total phenolic, flavonoids, and flavonol contents of rose wastewater and texture by-product extracts of *R. damascena*.

Source		Total phenolics		Total flavonoids		Total flavonols	
		Conc. (mg GAE/ g ext.)	%	Conc. (mg RE/ g ext.)	%	Conc. (mg QE/ g ext.)	%
Wastewater by-products (group A)	W ext.	48.27 ± 1.27[a]	4.82	16.68 ± 0.73[a]	1.66	8.47 ± 0.44[a]	0.84
	BW fr.	118.29 ± 2.92[b]	11.82	40.16 ± 1.05[b]	4.01	24.61 ± 0.75[b]	2.46
	AW fr.	14.74 ± 1.68[c]	1.47	2.25 ± 0.15[c]	0.22	1.35 ± 0.20[c]	0.13
Texture by-products (group B)	MT ext.	92.13 ± 4.18[a]	9.21	28.42 ± 0.63[a]	2.84	18.16 ± 0.81[a]	1.81
	BT fr.	230.69 ± 10.50[b]	23.06	71.66 ± 3.15[b]	7.16	51.70 ± 0.61[b]	5.17
	AT fr.	13.26 ± 2.21[c]	1.32	1.92 ± 0.07[c]	0.19	3.97 ± 0.26[c]	0.39

The results were expressed as mean ± standard deviation (SD) ($n = 3$); the lettering ([a, b, c]) indicated the significant difference ($p < 0.05$) in each group utilizing one-way analysis of variance (ANOVA, Tukey's *post hoc* test).
In group A: [a]Significant difference between W ext. and BW fr. & AW fr.; [b]Significant difference between BW fr. and W ext. & AW fr.;[c]Significant difference between AW fr. and W ext. & BW fr.
In group B: [a]Significant difference between MT ext. and BT fr. & AT fr.; [b]Significant difference between BT fr. and MT ext. & AT fr.; [c]Significant difference between AT fr. and MT ext. & BT fr.

Table 2. Assigned identification of chemical constituents of *R. damascena* wastewater and texture by-products by LC-ESI-MS in negative ion mode.

Comp. No.	t_R (minute)	Calcd. MW	$[M-H]^-$ *m/z*	MS fragments	Assigned identification	Source					
						MT	BT	AT	W	BW	AW
1	2.76	294	293	131, 113, 87	Methyl succinic acid -*O*-hexoside	+	+	−	+	+	−
2	3.00	192	191	173, 127, 93	Quinic acid	−	+	−	−	+	−
3	3.34	484	483	331, 169, 125	Digalloyl-*O*-hexoside	+	+	−	−	+	−
4	7.10	332	331	169, 125, 79	Galloyl-*O*-hexoside	−	−	−	+	+	−
5	7.77	170	169	125, 79	Gallic acid	+	−	−	+	+	−
6	8.27	484	483	331, 169, 125	Digalloyl-*O*-hexoside isomer	+	−	−	+	+	−
7	14.45	484	483	331, 169, 125	Digalloyl-*O*-hexoside isomer	+	+	+	+	+	+
8	16.78	346	345	183, 125, 79	M-H	+	−	−	−	−	−
9	18.04	634	633	481, 463, 301, 169	Galloyl- HHDP-hexoside	+	+	+	−	+	+
10	18.95	346	345	183, 125, 79	Methyl-gallate-*O*-hexoside isomer	+	+	+	+	+	+
11	20.96	786	785	483, 313, 169, 125	Digalloyl- HHDP-hexoside	−	+	−	−	+	−
12	22.13	484	483	331, 169, 125	Digalloyl-*O*-hexoside isomer	−	+	−	−	+	−
13	23.21	636	635	465, 313, 169, 125	Trigalloyl-*O*-hexoside	−	+	−	−	+	−
14	23.88	484	483	331, 169, 125	Digalloyl-*O*-hexoside isomer	−	+	−	−	+	−
15	24.63	332	331	169, 125, 79	Galloyl-*O*-hexoside isomer	−	+	−	−	+	−
16	25.47	786	785	635, 483, 313, 301, 169, 125	Digalloyl-HHDP-hexoside isomer	−	+	−	−	+	−
17	26.39	636	635	465, 313, 169, 125	Trigalloyl-*O*-hexoside isomer	−	+	−	+	+	−
18	27.47	446	445	345, 263, 221, 179, 113	Unknown	−	+	−	−	+	−
19	27.97	636	635	465, 313, 169, 125	Trigalloyl-*O*-hexoside isomer	−	+	−	+	+	−
20	28.47	584	583	451, 301, 271	Quercetin-*O*-(*O*-ferulyl) pentoside	−	+	+	−	+	+
21	28.90	786	785	635, 483, 313, 301, 169, 125	Digalloyl-HHDP--hexoside isomer	+	+	-	-	+	−
22	29.64	330	451	301, 271, 169, 79	Di-(*O*-Methyl) ellagic acid	−	−	−	−	+	−
23	30.48	452	451	301, 271, 151	Quercetin-*O*-galloyl	+	+	−	+	+	−
24	31.31	276	275	257, 229, 191	Unknown	+	+	−	+	+	−
25	31.81	592	591	411, 301, 169, 125	Ellagic acid derivatives	+	+	−	+	+	−
26	33.57	640	639	315, 151	Isorhamntin- di- *O*-hexoside	+	+	−	+	+	−
27	34.99	452	451	301, 271, 151	Quercetin-*O*-galloyl isomer	-		+	−	−	−
28	35.24	616	615	463, 301, 271, 179	Quercetin-*O*-(-*O*-galloyl)-hexoside	+	+	−	+	+	−
29	35.82	616	615	463, 301, 271, 179	Quercetin-*O*-(-*O*-galloyl)-hexoside isomer	+	+	−	+	+	−
30	36.66	434	433	301, 169, 125, 79	Ellagic acid-*O*-pentoside	-	+	−		+	−
31	37.24	610	609	463, 301, 151	Rutin	+	+	−	+	+	−
32	37.57	464	463	301, 151	Quercetin-*O*-hexoside	+	+	−	+	+	−
33	37.91	600	599	463, 301, 271, 151	Quercetin-*O*-hexose-protocatechoic acid	+	+	−	+	+	−
34	37.91	570	569	463, 301	Hydroxybenzyl- quercetin-*O*-hexoside	−	−	+	−	−	+
35	39.08	616	615	463, 301, 271, 179	Quercetin-*O*-(-*O*-galloyl)-hexoside isomer	+	+	-	+	+	−
36	39.99	508	607	545, 505, 463, 301, 271, 151	Quercetin-7-*O*-[3-hydroxy-3-methylglutaroyl] hexoside	+	+	−	+	+	−
37	40.41	600	599	447, 285, 151	Kaempferol-*O*-(-*O*-galloyl)-hexoside	+	+	−	+	+	−
38	40.58	436	435	271, 169	2-Phenylethyl 6-*O*-galloyl-β-D-glucopyranoside	+	+	−	+	+	−
39	40.66	610	609	435, 301, 151	Quercetin- derivative	+	+	−	+	+	−
40	41.67	448	447	285, 255, 151	Kaempferol-*O*-hexoside	+	+	−	+	+	−
41	42.92	600	599	447, 285, 151	Kaempferol-*O*-(-*O*-galloyl)-hexoside isomer	+	+	-	+	+	−
42	43.59	418	417	285, 255, 151	Kaempferol-*O*-pentoside	+	+	−	+	+	−

Continued

Comp. No.	t_R (minute)	Calcd. MW	[M-H]$^-$ *m/z*	MS fragments	Assigned identification	Source					
						MT	BT	AT	W	BW	AW
43	44.17	426	425	301, 271	Quercetin derivative	+	+	−	+	+	−
44	44.76	594	593	447, 285, 255, 151	Kaempferol-*O*-rutinoside	+	+	−	+	+	−
45	45.09	418	417	285, 255	Kaempferol-*O*-pentoside isomer	+	+	−	+	+	−
46	45.92	432	431	285, 255, 151	Kaempferol-*O*-deoxyhexoside	+	+	−	+	+	−
47	46.34	652	651	609, 447, 301, 151	Quercetin-*O*-(acetyl) rutinoside	+	+	−	+	+	−
48	47.93	610	609	463, 301, 271	Rutin isomer	+	+	−	+	+	−
49	49.34	636	635	593, 447, 285, 151	Kaempferol-*O*-(acetyl) rutinoside	+	+	−	+	+	−
50	49.77	302	301	179, 151	Quercetin	+	+		+	+	
51	50.43	636	635	593, 447, 285, 151	Kaempferol-*O*-(acetyl) rutinoside isomer	+	+	−	+	+	−
52	51.85	594	593	447, 285, 255, 151	Kaempferol-*O*-rutinoside isomer	+	+	−	+	+	−
53	54.61	583	582	462, 342	N',N'',N'''-tris-*p*-coumaroyl spermidine	+	+	−	−	+	−
54	56.03	286	285	169, 151	Kaempferol	+	+	−	+	+	−
55	57.61	288	287	269, 125	Eriodictyol	-	+	+	−	−	+

t_R: retention time; **Calcd. MW**: calculated molecular weight.

derived fractions, as shown in Table 2. The structures of the proposed identified compounds are shown in Figure 2; Figures 3 and 4 illustrate the LC-ESI-MS total ion chromatograms of Taif rose wastewater and texture extracts. In the present study, the compound number has been attributed to its elution time in all extracts.

Compound **1** was tentatively identified as methyl succinic acid-*O*-hexoside, which has an [M-H]$^-$ value at *m/z* 293, base peak at *m/z* 131, and other fragments at 113 and 87 (Ambati *et al*., 2019). Compounds **2** and **5** were assigned as quinic acid and gallic acid, respectively, by matching their deprotonated molecule and fragmentation pattern (Abdel-Hameed *et al*., 2013; Nowak *et al*., 2014).

Tannins were represented as one of the major constituents of *R. damascena* by-product extracts, including compounds **3, 6, 7, 12,** and **14**, which had a precursor ion peak at *m/z* 483 and characteristic product ions at *m/z* 331, 169, and 125 attributed to digalloyl-*O*-hexoside. Compounds **4** and **15** gave a pseudo molecular ion signal at *m/z* 331 and distinctive product ions at *m/z* 169, 125, and 79 corresponding to galloyl-*O*-hexoside (Abdel-Hameed *et al*., 2013; Riffault *et al*., 2014). In addition, compounds **8** and **10** were tentatively characterized as methyl-gallate-*O*-hexoside due to the existence of the [M-H]$^-$ ion at *m/z* 345 and fragment ions at *m/z* 183, 125 and 79 (Stanila *et al*., 2015). Compound **9** showed a pseudo molecular ion signal [M-H]$^-$ at *m/z* 633 and other fragments at *m/z* 481, 463, and 301, which coincided with a galloyl-HHDP-hexoside (Carocho *et al*., 2014). Compounds **11, 16,** and **21** possessed a deprotonated molecule at *m/z* 785 [M-H]$^-$ and other fragments at *m/z* 483, 313, 169, and 125, which are characteristics of digalloyl-HHDP-hexoside (Abdel-Hameed *et al*., 2013; Peršurić *et al*., 2020). Compounds **13, 17,** and **19** exhibited the deprotonated molecular ion at *m/z* 635 [M-H]$^-$ with specific fragment ions at *m/z* 465, 313, 169, and 125. Hence, it was identified as trigalloyl- *O*-hexoside (Carocho *et al*., 2014). Compound **20** represented [M-H]$^-$ ion peak at *m/z* 583, afforded fragments at *m/z* 451[M-H-132]$^-$ and *m/z* 301 [M-H-132-151]$^-$, which indicated the loss of pentoside and galloyl units, respectively. So, compound 20 was tentatively characterized as quercetin-(*O*-galloyl)-*O*-pentoside. Compound **22** was identified as di-*O*-methyl-ellagic acid by its characteristic [M-H]$^-$ at *m/z* 329 and other fragments at *m/z* 301, 271, 169, and 79. Compound **30** had [M-H]$^-$ at *m/z* 433 and a base peak at *m/z* 301 of ellagic acid. Therefore, compound **30** was deduced as ellagic acid-*O*-pentoside (Singh *et al*., 2016). In addition, compound 25 was tentatively identified as an ellagic acid derivative.

The second major phytoconstituents group were flavonoids, including compound **20**, which had [M-H]$^-$ ion peak at *m/z* 583, product ions at *m/z* 451 [M-H- 132]$^-$ and a base peak of quercetin at 301 [M-H- 132-150]$^-$ corresponding to the loss of pentoside and ferulic acid moieties, respectively. Therefore, compound **20** was characterized as quercetin-*O*-(*O*-feruloyl) pentoside. Compounds **23** and **27** afforded the same [M-H]$^-$ ion at *m/z* 451 and other fragments at *m/z* 301, 271, and 151, which are relatives of quercetin-*O*-galloyl. Compound **26** showed a pseudo molecular ion peak at *m/z* 639 [M-H]$^-$ and a fragment ion at *m/z* 315 [M-H-324]$^-$ due to the loss of two hexose units. Therefore, compound **26** was identified as isorhamnetin-di-*O*-hexosides (El-Hagrassy *et al*., 2017). Compounds **28**, **29**, and **35** had a precursor ion at *m/z* 615 [M-H]$^-$. The second-generation product ion generated the product ions at *m/z* 463 [M-H- 152]$^-$, *m/z* 301 [M-H-152-162]$^-$ due to the elimination of galloyl and hexoside units, respectively. Such a fragmentation pattern confirmed the presence of quercetin-*O*-(*O*-galloyl)-hexoside (Saldanha *et al*., 2013). Compounds **31** and **48** were tentatively identified as rutin with a characteristic [M-H]$^-$ ion peak at *m/z* 609 and product ions at *m/z* 463, 301, and 151, respectively. Compound **32** had [M-H]$^-$ an ion peak at *m/z* 463 and fragment ions at 301 and 151, which are relatives of quercetin-*O*-hexoside. Also, compound **33** had an [M-H]$^-$ at *m/z* 599 and other signals at *m/z* 463 [M-H-136]$^-$, which come from the demise of a protocatechuic acid unit (*m/z* 301, 271, 151). Hence, compound 33 was tentatively characterized as quercetin-*O*-hexose-protocatechuic acid (Abdel-Hameed *et al*., 2013). Compound **34** exhibited [M-H]$^-$ at *m/z* 569 and after losses

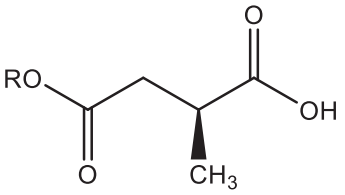

1. R= hexose

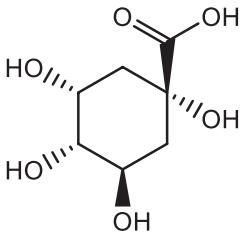

2

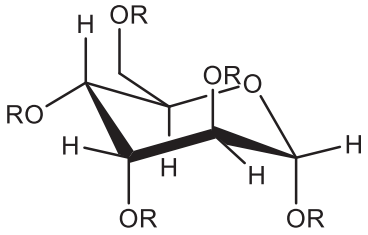

3. Two Rs= Galloyl three Rs= H
4. One R= Galloyl four Rs= H
13. Three Rs= Galloyl two Rs= H

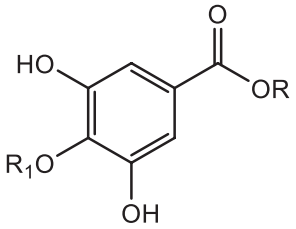

5. R= H R_1= H
8. R= Me R_1= hexoside

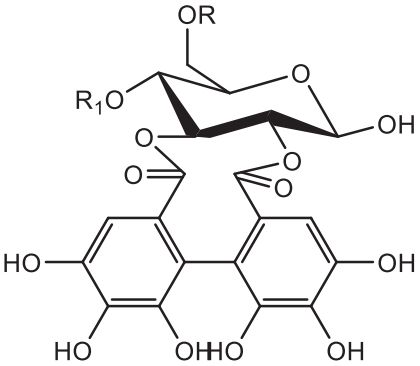

9. R= galloyl R_1= H
11. R= galloyl R_1= galloyl

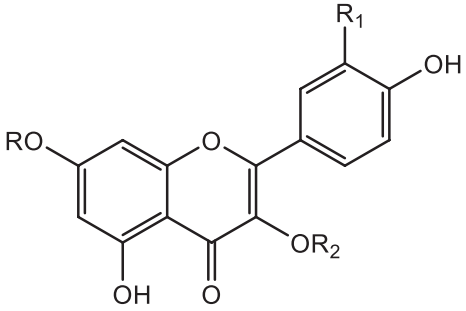

	R	R_1	R_2
20.	H	OH	(ferulyl)-pentoside
23.	H	OH	galloyl
28.	H	OH	(galloyl)-hexoside
31.	H	OH	rutinoside
32.	H	OH	hexoside
33.	H	OH	hexose-protocatechoic acid
34.	H	OH	hydroxybenzyl-*O*-hexoside
37.	H	H	(galloyl)-hexoside
40.	H	H	hexoside
42.	H	H	pentoside
44.	H	H	rutinoside
46.	H	H	deoxyhexoside
47.	H	OH	acetyl-rutinoside
49.	H	H	acetyl-rutinoside
50.	H	OH	H
54.	H	H	H

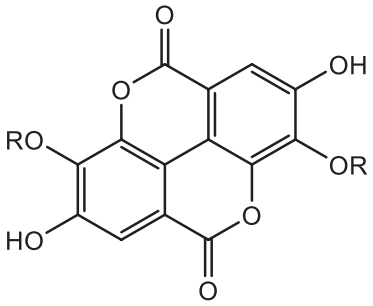

22. two Rs= Me
30. one R= H one R= pentoside

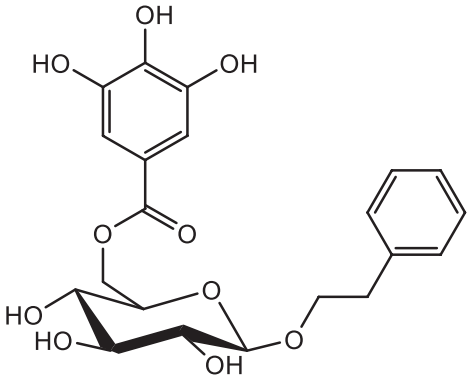

38

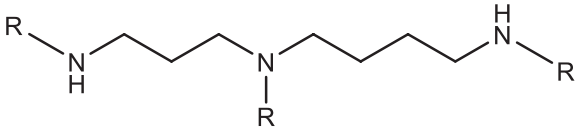

53. R= coumaroyl

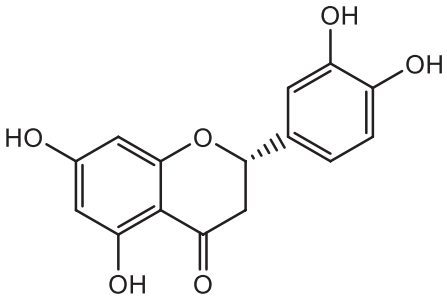

55

Figure 2. Chemical structures of compounds of interest in *R. damascena* wastewater and texture by-products.

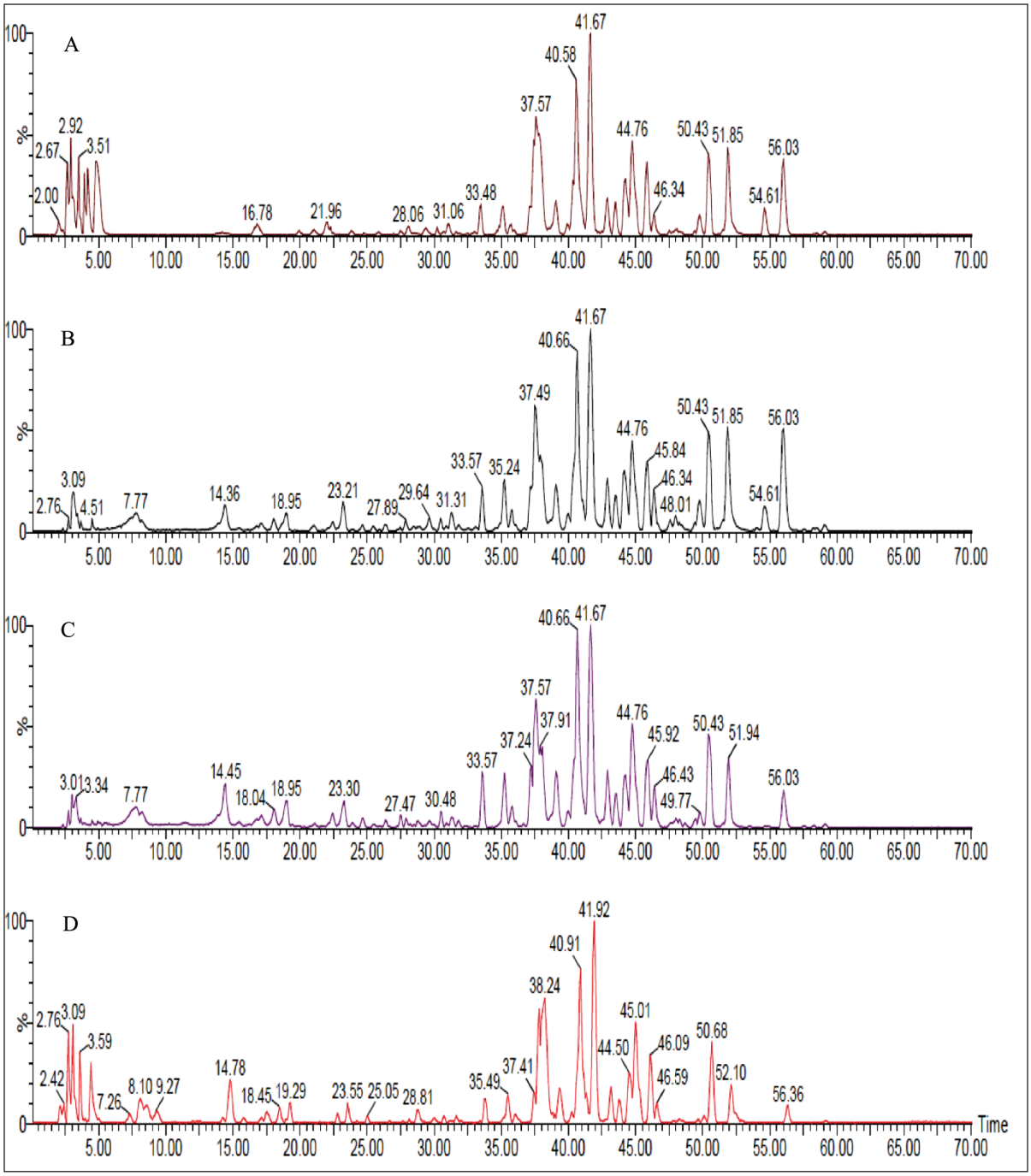

Figure 3. LC-ESI-MS total ion chromatograms of *R. damascena* wastewater and texture extracts; (A) MT extract, (B) BT fraction, (C) BW fraction, and (D) W extract at the negative ion mode.

of hydroxybenzyl (106 Da) and hexoside (162 Da) units, it yielded a fragment ion at *m/z* 301 (quercetin). Therefore, it was identified as hydroxybenzyl-quercetin-*O*-hexoside (Lee *et al*., 2009). Compound **36** afforded $[M-H]^-$ ion peak at *m/z* 607 that produced other ions at *m/z* 545 and 505, which revealed the loss of H_2O and CO_2, respectively. Further fragments appeared at *m/z* 463 and 301 of the quercetin aglycone and liberation of 144 Da (3-hydroxy-3-methylglutaroyl) and 162 Da (hexose), respectively. Therefore, compound **36** was characterized as quercetin-7-*O*-[3-hydroxy-3-methylglutaroyl]-hexoside and reported in *R. spinosissima* L. (López-Angulo *et al*., 2018; Porter *et al*., 2012). Compound **47** had a molecular ion signal at *m/z* 651 $[M-H]^-$ and fragment ions at *m/z* 609 $[M-H-42]^-$, *m/z* 447 $[M-H-42-162]^-$, and *m/z* 301$[M-H-42-162-146]^-$, which means a neutral loss of acetyl group, hexose, and deoxyhexose units, respectively. Therefore, compound **47** was assigned as quercetin-*O*-(acetyl)-rutinoside. Moreover, compound **50** had $[M-H]^-$ ion peak at 301 and characteristic fragments at *m/z* 179 and 151 of quercetin aglycone (Jang *et al*., 2018).

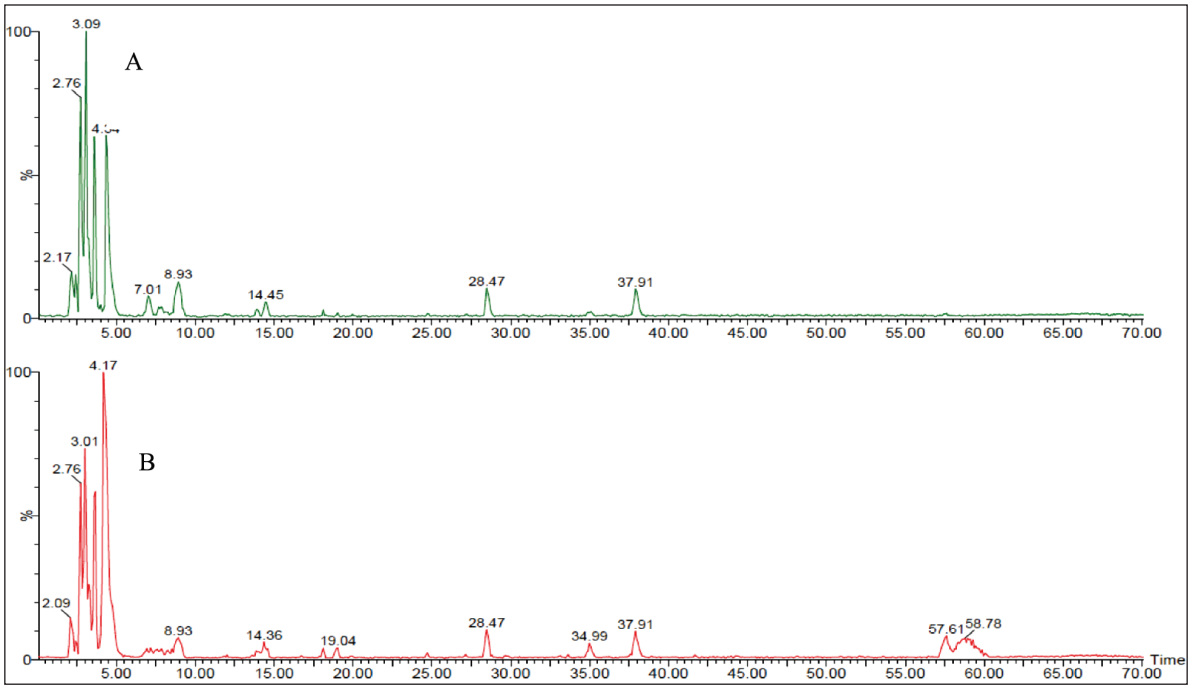

Figure 4. LC-ESI-MS total ion chromatograms of *R. damascena* wastewater and texture extracts: (A) AW fraction and (B) AT fraction at the negative ion mode.

Compounds **37** and **41** showed deprotonated molecules at *m/z* 599 $[M-H]^-$. The second-generation product ion was responsible for creating the product ions at *m/z* 447 [M-H-152 (galloyl)]$^-$, *m/z* 285 [M-H 152(galloyl)- 162(hexose)]$^-$. Thus, it was characterized as kaempferol-*O*-(*O*-galloyl)-hexoside. Compound **40** gave deprotonated molecule at *m/z* 447 $[M-H]^-$ and other fragments at *m/z* 285 [M-H-162]$^-$, 255, and 151, which are characteristics of kaempferol-*O*-hexoside. Compounds **42** and **45** had $[M-H]^-$ ion peak at *m/z* 417 and base peak at *m/z* 285 (kaempferol). Thus, these two compounds were identified as kaempferol-*O*-penoside and its isomer, respectively. Compounds **44** and **52** had an $[M-H]^-$ ion peak at *m/z* 593 and other fragments at *m/z* 447 and *m/z* 285, revealing loss of deoxyhexose and hexoside units. Therefore, the two compounds were identified as kaempferol-*O*-rutinoside and its isomer, respectively. Compound **46** was identified as kaempferol-*O*-deoxyhexoside because it had an $[M-H]^-$ at *m/z* 431 and a base peak at *m/z* 285. Compounds **49** and **51** showed an $[M-H]^-$ ion peak at *m/z* 635 and other signals at *m/z* 593 [M-H-42 (acetyl group)], *m/z* 447 [M-H-42 (acetyl group)-146 (deoxyhexose)] and *m/z* 285 [M-H-42 (acetyl group)-146 (deoxyhexose)-162 (hexose)]. Therefore, the two compounds were identified as kaempferol-*O*- (acetyl) rutinoside and its isomer, respectively. In addition, compound **54** was identified as kaempferol (aglycone) with an $[M-H]^-$ at *m/z* 285 (Mohsen *et al*., 2020; Dina *et al*., 2021). Compound **55** was classified as a flavanone compound with $[M-H]^-$ at *m/z* 287 and characteristic product ions at *m/z* 269 and 151 of eriodictyol (Zhang *et al*., 2007).

Other compounds include compound **38,** which afforded an $[M-H]^-$ ion peak at *m/z* 435 and characteristic fragments at *m/z* 271 and 169 of 2-phenylethyl 6-*O*-galloyl-β-D-glucopyranoside. Compound **38** has previously been isolated from the flowers of *R. damascena* (Elkhateeb *et al*., 2007; Dina *et al*., 2021). Compound **53** exhibited an $[M-H]^-$ at *m/z* 582 and different fragments at *m/z* 462 and 342 due to the liberation of a coumaric acid. Therefore, it was characterized as N', N", N"'-tris-p-coumaroyl spermidine, which is classified as hydroxycinnamic acid amide (Negri *et al*., 2018).

The previous phytochemical investigation reports of Bulgarian and Taif roses have proved the detection of different mono-, di-, and acylated glycosides of ellagic acid, gallic acid, catechin, quercetin, kaempferol, and their derivatives (Gateva *et al*., 2022). In addition, some derivatives of quercetin, kaempferol, and ellagic acid were isolated and characterized from Bulgarian rose wastewater, as reported by Solimine *et al*. (2016). Furthermore, over 60 compounds were detected in the wastewater of the four Bulgarian *Rosa* species (*R. damascena* Mill., *R. alba* L., *R. gallica* L., and *R. centifolia* L), most of them are flavonoids, ellagic, gallic acids, catechin, epicatechin, and their derivative (Georgieva *et al*., 2021). Herein, six compounds were reported for the first time in rose extracts including methyl succinic acid–hexoside, di-(*O*-Methyl) ellagic acid, hydroxybenzyl- quercetin-*O*-hexoside, quercetin-7-*O*-[3-hydroxy-3-methylglutaroyl] hexoside, N', N", N"'-tris-*p*-coumaroyl spermidine, and eriodictyol.

Antioxidant activity

In this study, three methods were carried out, including the FRP and phosphomolybdenum assays which are based on a single-electron transfer mechanism, while DPPH radical assay is based on radical scavenging (H transfer). The FRP mechanism cannot detect the antioxidants that can be detected by DPPH radical. Thus, the reduction of Fe^{3+} and Mo (VI), as well as the formation of their complexes, is really important since when they

Table 3. Total antioxidant capacity, FRP activity, and DPPH free radical scavenging activity of *R. damascena* wastewater and texture by-product extracts.

Extract		Total antioxidant capacity [mg AAE /g ext.]	FRP activity [mg AAE/g ext.]	DPPH free radical scavenging activity SC_{50} [µg/ml]
Wastewater by-products (group A)	W ext.	309.21 ± 9.05[a]	207.24 ± 1.87[a]	34.25 ± 0.49[a]
	BW fr.	380.22 ± 13.17[b]	359.23 ± 3.28[b]	12.78 ± 0.13[b]
	AW fr.	60.83 ± 10.06[c]	66.46 ± 2.70[c]	>100[c]
Texture by-products (group B)	MT ext.	392.90 ± 9.56[a]	254.26 ± 5.81[a]	17.79 ± 0.10[a]
	BT fr.	518.37 ± 25.31[b]	513.63 ± 4.25[b]	7.57 ± 0.01[b]
	AT fr.	138.15 ± 11.61[c]	107.02 ± 1.56[c]	>100[c]
Ascorbic acid				5.83 ± 0.24

The results were expressed as mean ± standard deviation (SD) ($n = 3$); the lettering ([a, b, c]) indicated the significant difference ($p < 0.05$) in each group utilizing one-way analysis of variance (ANOVA, Tukeys *post hoc* test).

In group A: [a]significant difference between W ext. and BW fr. & AW fr.; [b]significant difference between BW fr. and W ext. & AW fr.; [c]significant difference between AW fr. and W ext. & BW fr.

In group B: [a]significant difference between MT ext. and BT fr. & AT fr.; [b]significant difference between BT fr. and MT ext. & AT fr.; [c]significant difference between AT fr. and MT ext. & BT fr.

are in a "free" state, they can catalyze the production of hydroxyl radicals which consider highly toxic radicals (Zhu *et al*., 2011).

DPPH radical scavenging activity

The stable free radical DPPH has an absorption band at 517 nm. It can lose this absorption by taking in an electron or a certain type of free radical, which results in a visual shift from purple to yellow color. One of its advantages is that it can accommodate many samples in a short time with high sensitivity to record the active ingredients at low concentrations (Qingming *et al*., 2010). In the present study, all of the by-product extracts exhibited DPPH radical scavenging properties. This was observed by the low SC_{50} value, which indicates a higher antioxidant activity (Table 3). The BT and BW fractions had significant SC_{50} values of 7.57 ± 0.01 and 12.78 ± 0.13 µg/ml, respectively. The MT and W extracts showed higher SC_{50} values (SC_{50} = 17.79 ± 0.10 and 34.25 ± 0.49 µg/ml, respectively), while the AT and AW fractions had a low antiradical scavenging activity with a value of >100 µg/ml. In addition, ascorbic acid was used as standard and represented a powerful antiradical activity with an SC_{50} value of 5.83 ± 0.24 µg/ml. It was reported that the DPPH assay is applicable to hydrophobic systems like highly pigmented plants, such as roses, cherries, and red cabbage (Floegel *et al*., 2011). Therefore, the results of tested extracts of *R. damascene* showed a significant DPPH radical scavenging activity, especially BT and BW fractions.

FRP assay

This assay monitoring the reduction of Fe^{3+} to Fe^{2+} was used to determine the extracts' FRP. Depending on the FRP of the tested samples, the test solution's yellow hue changes to green or blue in this assay. Antioxidant-containing materials result in the reduction of the Fe^{3+}/ferricyanide complex to the Fe^{2+} form, which can be observed by measuring the appearance of Perl's Prussian blue at 700 nm (Georgieva *et al*., 2021). The results in Table 3 showed that the BT and BW fractions had a good metal-reducing capacity (513.63 ± 4.25 and 359.23 ± 3.28 mg AAE /g ext., respectively), followed by the MT and W extracts (254.26 ± 5.81 and 207.24 ± 1.87 mg AAE /g ext., respectively). However, the aqueous fractions of both AT and AW showed the lowest metal-reducing power with a value of 107.02 ± 1.56 and 66.46 ± 2.70 mg AAE /g ext., respectively). Therefore, the tested extracts and fractions afforded some degree of electron donating capacity in a concentration-dependent manner. It was reported that an FRP of the aqueous extract of *R. damascena* had 5.08 ± 0.07 mmol Fe^{2+}/g (Dudonné *et al*., 2009). On the other hand, the hydroethanolic extract of the Moroccan *R. damascena* flowers displayed 0.20 ± 0.1 mg/ml (Chroho *et al*., 2022).

Phosphomolybdenum assay

The phosphomolybdenum assay or total antioxidant capacity (TAC) method is based on the reduction of Mo (VI) of ammonium molybdate to Mo (V) to form a green subsequent of phosphate/Mo (V) complex at acidic pH (Abdel-Hameed *et al*., 2009). In this study, the reduction effect of examined extracts and fractions were arranged in the following order BT fraction with the value of 518.37 ± 25.31 mg AAE /g ext. > BW fraction (392.90 ± 9.56 mg AAE /g ext.) > MT extract (380.22 ± 13.17 mg AAE /g ext.) > W extract (309.21 ± 9.05 mg AAE /g ext.) > AT fraction (138.15 ± 11.61mg AAE /g ext.) > AW fraction (60.83 ± 10.06 mg AAE /g ext.) as shown in Table 3. These results suggest the powerful electron donating properties of BT and BW fractions with a large metal reduction capacity. Moreover, our results demonstrated a close correlation exists between the polarity of the extracting solvent and the content of active ingredients.

The previous studies reported that the TAC of the hydroethanolic extract from *R. damascene* flowers was 213.22 mg AAE/ g extract (Chroho *et al*., 2022). In addition, the ethanolic extract of fresh and spent flowers of *R. damascena* showed TAC with values of 372.26 ± 0.96 to 351.36 ± 0.84 mg/g extract (Ozkan *et al*., 2004). Indeed, our study showed that the extract from *R. damascena* flowers exhibited a powerful TAC, which may be due to the presence of phenolic compounds.

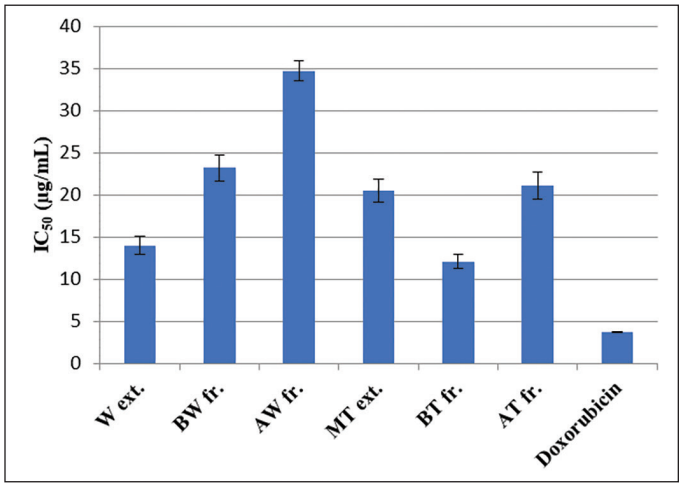

Figure 5. IC_{50} of tested *R. damascena* wastewater and texture extracts toward the HepG2 cell line.

The anticancer activity

Environmental, chemical, physical, metabolic, and genetic variables all play a part in the development and progression of cancer in a multi-step process (Gomaa, 2013). There are so many kinds of cancers that affect the human body, among them hepatocellular carcinoma, which is considered the fourth leading cause of all deaths worldwide. For a variety of causes, including alcoholism, hepatitis B virus, hepatitis C virus, hemochromatosis, type 2 diabetes, hemophilia, and oxidative stress, it typically develops in the backdrop of cirrhosis (Barmoudeh *et al*., 2022; Ly *et al*., 2021). Cancer therapies frequently employ natural ingredients, particularly those derived from plants. The newly proposed idea of a broad-spectrum integrative approach to cancer prevention and therapy is based on the fact that they contain a wide range of bioactive secondary metabolites (Al-Dabbagh *et al*., 2018). Herein, the effects of *R. damascena* by-products were investigated against the HepG2 cell line and doxorubicin was used as a positive control (Fig. 5). The results revealed that the BT fraction showed the highest potent anticancer activity (IC_{50} = 12.1 ± 0.85 µg/ml), followed by the W extract (14.00 ± 1.05 µg/ml), MT extract (20.5 ± 1.41 µg/ml), and AT fraction (21.1 ± 1.6441 µg/ml). The BW and AW fractions exhibited the lowest IC_{50} value of 23.2 ± 1.57 and 34.7 ± 1.18 µg/ml, respectively. In contrast, doxorubicin had IC_{50}= 3.73 ± 0.09 µg/ml. A previous study carried out by Gateva *et al*. (2022) reported that *R. damascena* wastewater fraction has a cytoprotective effect and is toxic at concentrations of 100 µg/ml and higher in HepG2 cells using the (3-[4,5-dimethylthiazol-2-yl]-2,5 diphenyl tetrazolium assay (Gateva *et al*., 2022). Thus, the potent anticancer activity of *R. damascena* industrial by-product extracts may be due to the presence of high levels of polyphenolic compounds.

CONCLUSION

In summary, the current study demonstrated that the industrial by-product extracts of *R. damascena* contain high levels of phenolic, flavonoids, and flavonol contents, especially for BT fr., BW fr., and MT extract, respectively. The LC-ESI-MS analysis led to identifying of 55 polyphenolic compounds in the tested extracts classified as organic acids, phenolic acids, tannins, and flavonoids. Furthermore, the BT and BW fractions had a high DPPH radical scavenging activity (SC_{50} = 7.57 ± 0.01 and 12.78 ± 0.13 µg/ml, respectively), which is near to the value of ascorbic acid (SC_{50} = 5.83 ± 0.24 µg/ml) as well as in the two other *in vitro* assays. Also, they exhibited a high inhibition activity of HepG2 cells (IC_{50} = 12.1 ± 0.85 and 14.00 ± 1.05 µg/ml, respectively). Thus, the reuse of *R. damascena* by-products will not only provide significant environmental benefits but also will contribute to evaluating their extracts with potential applications in pharmaceutical industries.

AUTHORS CONTRIBUTIONS

Ezzat E. A. Osman designed and performed the experiments analyzed and interpreted the data and results, the original manuscript. Salih A. Bazaid provided instrument facilities and revised the manuscript. El-Sayed S. Abdel-Hameed designed the experiments and wrote and revised the original manuscript.

CONFLICTS OF INTEREST

The authors declare no conflicts of interest.

FINANCIAL SUPPORT

This research did not receive any specific grant from funding agencies in the public, commercial, or not- for- profit sectors.

ETHICAL APPROVALS

This study does not involve experiments on animals or human subjects.

DATA AVAILABILITY

The datasets generated during and/or analyzed during the current study are available from the corresponding author upon reasonable request.

PUBLISHER'S NOTE

This journal remains neutral with regard to jurisdictional claims in published institutional affiliation.

REFERENCES

Abdel-Hameed ES, Bazaid SA, Hagag HA. Chemical characterization of *Rosa damascena* Miller var. *trigintipetala* Dieck essential oil and its *in-vitro* genotoxic and cytotoxic properties. J Essen Oil Res, 2016; 28:121–9; doi:10.1080/10412905.2015.1099120

Abdel-Hameed ES, Bazaid SA, Salman MS. Characterization of the phytochemical constituents of Taif rose and its antioxidant and anticancer activities. Biomed Res Int, 2013; 2013:345465; doi:10.1155/2013/345465

Abdel-Hameed ES, Bazaid, SA, Sabra AA. Total phenolic, *in vitro* antioxidant activity and safety assessment (acute, sub-chronic and chronic toxicity) of industrial Taif rose water by-product in mice. Der Pharm Lett, 2015; 7:251–9.

Abdel-Hameed ES. Total phenolic contents and free radical scavenging activity of certain Egyptian *Ficus* species leaf samples. Food Chem, 2009; 114:1271–7; doi:10.1016/j.foodchem.2008.11.005

Al-Dabbagh B, Elhaty IA, Al Hrout A, Al Sakkaf R, El-Awady R, Ashraf SS, Amin A. Antioxidant and anticancer activities of *Trigonella foenum-graecum, Cassia acutifolia and Rhazya stricta*. BMC Complement Altern Med, 2018; 18:240; doi:10.1186%2Fs12906-018-2285-7

Ambati CR, Vantaku V, Donepudi SR, Amara CS, Ravi SS, Mandalapu A, Perla M, Putluri V, Sreekumar A, Putluri N., Measurement of methylated metabolites using liquid chromatography-mass spectrometry and its biological application. Anal Methods, 2019; 11:49–57; doi:10.1039/c8ay02168f

Barmoudeh Z, Ardakani MT, Doustimotlagh AH, Bardania H. Evaluation of the antioxidant and anticancer activities of hydroalcoholic extracts of *Thymus daenensis* Čelak and *Stachys pilifera* Benth. J Toxicol, 2022; 30:1924265; doi:10.1155/2022/1924265

Baydar NG, Baydar H. Phenolic compounds, antiradical activity and antioxidant capacity of oil-bearing rose (*Rosa damascena* Mill.) extracts. Indus Crops Prod, 2013; 41:375–80; doi:10.1016/j.indcrop.2012.04.045

Carocho M, Barros L, Bento A, Santos-Buelga C, Morales P, Ferreira IC. *Castanea sativa* Mill. flowers amongst the most powerful antioxidant matrices: a phytochemical approach in decoctions and infusions. BioMed Res Int, 2014; 2014:232956; doi:10.1155/2014/232956

Chroho M, Bouymajane A, Oulad El Majdoub Y, Cacciola F, Mondello L, Aazza M, Zair T, Bouissane L. Phenolic Composition, Antioxidant and antibacterial activities of extract from flowers of *Rosa damascena* from Morocco. Separations, 9; 2022:247; https://doi.org/10.3390/separations9090247

Dina E, Sklirou AD, Chatzigeorgiou S, Manola MS, Cheilari A, Louka XP, Argyropoulou A, Xynos N, Skaltsounis AL, Aligiannis N, Trougakos IP. An enriched polyphenolic extract obtained from the by-product of *Rosa damascena* hydrodistillation activates antioxidant and proteostatic modules. Phytomedicine, 2021; 93:153757; doi: 10.1016/j.phymed.2021.153757

Dobreva A, Getchovska K, Nedeltcheva-Antonova D. A comparative study of Saudi Arabia and Bulgarian rose oil chemical profile: The effect of the technology and geographic origin. Flavour Fragr J, 2020; 35:584–96; doi:10.1002/ffj.3601

Dudonné S, Vitrac X, Coutière P, Woillez M, Mérillon J-M. Comparative study of antioxidant properties and total phenolic content of 30 plant extracts of industrial interest using DPPH, ABTS, FRAP, SOD, and ORAC assays. J Agric Food Chem. 2009; 57:17681774; https://doi.org/10.1021/jf803011r

El-Hagrassy AM, Elkhateeb A, Hussein SR, Abdel-Hameed ES, Marzouk MM. LC-ESI-MS profile, antioxidant activity and cytotoxic screening of *Oligomeris linifolia* (Vahl) Macbr. (Resedaceae). J Appl Pharm Sci, 2017; 7:043–7; doi:10.7324/JAPS.2017.70807

Elkhateeb A, Matsuura H, Yamasaki M, Maede Y, Katakura K, Nabeta K. Anti-Babesial compounds from *Rosa damascena* Mill. Nat Prod Commun, 2007; 2:765–9.

Erbaş S, Baydar H. Variation in Scent Compounds of Oil-Bearing Rose (*Rosa damascena* Mill.) Produced by headspace solid phase microextraction, hydrodistillation and solvent extraction. Rec Nat Prod, 2016; 10:555–65.

Floegel A, Kim D-O, Chung S-J, Koo SI, Chun OK. Comparison of ABTS/DPPH assays to measure antioxidant capacity in popular antioxidant-rich US foods. J Food Compos Anal, 2011; 24:1043–8; https://doi.org/10.1016/j.jfca.2011.01.008

Gateva S, Jovtchev G, Angelova T, Dobreva A, Mileva M. The Anti-Genotoxic activity of wastewaters produced after water-steam distillation of Bulgarian *Rosa damascena* Mill. and *Rosa alba* L. essential oils. Life, 2022; 12:455; doi:10.3390/life12030455

Georgieva A, Ilieva Y, Kokanova-Nedialkova Z, Zaharieva MM, Nedialkov P, Dobreva A, Kroumov A, Najdenski H, Mileva M. Redox-modulating capacity and antineoplastic activity of wastewater obtained from the distillation of the essential oils of four Bulgarian oil-bearing roses. Antioxidants, 2021; 10:1615; doi:10.3390/antiox10101615

Gerasimova T, Topashka-Ancheva, M, Dobreva A, Georgieva A, Mileva M. Evaluation of the genotoxic activity of wastewater obtained after steam distillation of essential oil of Bulgarian *Rosa alba* L. *in vivo* study. Rom Biotechnol Lett, 2022; 27:3292–301; doi:10.25083/rbl/27.1/3292-3301

Gomaa EZ. *In vitro* Antioxidant, Antimicrobial, and antitumor activities of bitter almond and sweet apricot (*Prunus armeniaca* L.) kernels. Food Sci Biotech, 2013; 22:455–63; doi:10.1007/s10068-013-0101-1

Hagag HA, Bazaid SA, Abdel-Hameed ES, Salman M. Cytogenetic, cytotoxic and GC-MS studies on concrete and absolute oils from Taif rose, Saudi Arabia. Cytotechnology, 2014; 66:913–23; doi:10.1007%2Fs10616-013-9644-5

Harjumäki R, Nugroho RWN, Zhang X, Lou Y-R, Yliperttula M, Valle-Delgado JJ, Österberg M. Quantified forces between HepG2 hepatocarcinoma and WA07 pluripotent stem cells with natural biomaterials correlate with *in vitro* cell behavior. Sci Rep, 2019; 9:7354; https://doi.org/10.1038/s41598-019-43669-7

Ilieva Y, Dimitrova L, Georgieva A, Vilhelmova-Ilieva N, Zaharieva MM, Kokanova-Nedialkova Z, Dobreva A, Nedialkov P, Kussovski V, Kroumov AD, Najdenski H, Mileva M. *In vitro* study of the biological potential of wastewater obtained after the distillation of four Bulgarian oil-bearing Roses. Plants, 2022; 11:1073; doi:10.3390/plants11081073

Jang GH, Kim HW, Lee MK, Jeong SY, Bak AR, Lee DJ, Kim JB. Characterization and quantification of flavonoid glycosides in the *Prunus* genus by UPLC-DAD-QTOF/MS. Saudi J Biol Sci, 2018; 25:1622–31; doi: 10.1016/j.sjbs.2016.08.001

Kumar N, Bhandari P, Singh B, Gupta AP, Kaul VK. Reversed phase-HPLC for rapid determination of polyphenols in flowers of rose species. J Sep Sci, 2008; 31:262–7; doi:10.1002/jssc.200700372

Lee YJ, Kim S, Lee SJ, Ham I, Whang WK. Antioxidant activities of new flavonoids from *Cudrania tricuspidata* root bark. Arch Pharm Res, 2009; 32(2):195–200; doi:10.1007/s12272-009-1135-z

López-Angulo G, Montes-Avila J, Díaz-Camacho SP, Vega-Aviña R, López-Valenzuela JA, Delgado-Vargas F. Comparison of terpene and phenolic profiles of three wild species of *Echeveria* (Crassulaceae). J Appl Bot Food Qual, 2018; 91:145–54; doi:10.5073/JABFQ.2018.091.020

Ly HT, Truong TM, Nguyen TH, Nguyen HD, Zhao Y, Le VM. Phytochemical screening and anticancer activity of the aerial parts extract of *Xanthium strumarium* L. on HepG2 cancer cell line. Clin Phytosci, 2021; 7:14; doi:10.1186/s40816-021-00252-w

Mohsen E, Younis IY, Farag MA. Metabolites profiling of Egyptian *Rosa damascena* Mill. flowers as analyzed via ultra-high-performance liquid chromatography-mass spectrometry and solid-phase microextraction gas chromatography-mass spectrometry in relation to its anti-collagenase skin effect. Indus Crops Prod, 2020; 155:112818; doi:10.1016/j.indcrop.2020.112818

Negri G, Barreto LMRC, Sper FL, de Carvalho C, Campos MGR. Phytochemical analysis and botanical origin of *Apis mellifera* bee pollen from the municipality of Canavieiras, Bahia State, Brazil. Braz J Food Tech, 2018; 21:e2016176; doi:10.1590/1981-6723.17616

Nowak R, Olech M, Pecio L, Oleszek W, Los R, Malm A, Rzymowska J. Cytotoxic, antioxidant, antimicrobial properties and chemical composition of rose petals. J Sci Food Agric, 2014; 94:560–7; doi:10.1002/jsfa.6294

Osman EEA, Mohamed AS, Elkhateeb A, Gobouri A, Abdel-Aziz MM, Abdel-Hameed ES. Phytochemical investigations, antioxidant, cytotoxic, antidiabetic and antibiofilm activities of *Kalanchoe laxiflora* flowers. Eur J Integr Med, 2022; 49:102085; doi:10.1016/j.eujim.2021.102085

Özkan G, Sagdiç O, Baydar NG, Baydar H. Note: antioxidant and antibacterial activities of *Rosa damascena* flower extracts. Food Sci Technol Int, 2004; 10:277–81; https://doi.org/10.1177/108201320404588

Peršurić Ž, Saftić ML, Malenica M, Gobin I, Pedisić S, Dragović-Uzelac V, Kraljević PS. Assessment of the Biological Activity and Phenolic Composition of Ethanol Extracts of Pomegranate (*Punica granatum* L.) Peels. Molecules, 2020; 25:5916; doi:10.3390/molecules25245916

Porter EA, van den Bos, AA, Kite GC, Veitch NC, Simmonds MS. Flavonol glycosides acylated with 3-hydroxy-3-methylglutaric acid as systematic characters in Rosa. Phytochem, 2012; 81:90–6; doi: 10.1016/j.phytochem.2012.05.006

Prieto P, Pineda M, Aguilar M. Spectrophotometric quantitation of antioxidant capacity through the formation of a phosphomolybdenum complex: specific application to the determination of vitamin E. Anal Biochem, 1999; 269:337–41; doi:10.1006/abio.1999.4019

Qingming Y, Xianhui P, Weibao K, Hong Y, Yidan S, Li Z, Yanan Z, Yuling Y, Lan D, Guoan L. Antioxidant activities of malt extract from barley (*Hordeum vulgare* L.) toward various oxidative stress *in vitro* and *in vivo*. Food Chem, 2010; 118:84–9; doi: 10.1016/j.foodchem.2009.04.094

Riffault L, Destandau E, Pasquier L, André P, Elfakir C. Phytochemical analysis of *Rosa hybrida* cv. 'Jardin de Granville' by HPTLC, HPLC-DAD and HPLC-ESI-HRMS: polyphenolic fingerprints of six plant organs. Phytochem, 2014; 99:127–34; doi: 10.1016/j.phytochem.2013.12.015

Rusanov K, Garo E, Rusanova M, Fertig O, Hamburger M, Atanassov I, Butterweck V. Recovery of polyphenols from rose oil distillation wastewater using adsorption resins–a pilot study. Planta Med, 2014; 80:1657–64; doi:10.1055/s-0034-1383145

Sabahi A, Farmani F, Mousavinoor E, Moein M. Valorization of waste water of *Rosa damascena* oil distillation process by ion exchange chromatography. Sci World J, 2020; 30:5409493; doi:10.1155/2020/5409493

Saldanha LL, Vilegas W, Dokkedal AL, Characterization of flavonoids and phenolic acids in *Myrcia bella* Cambess. using FIA-ESI-IT-MS(n) and HPLC-PAD-ESI-IT-MS combined with NMR. Molecules, 2013; 18:8402–16; doi:10.3390/molecules18078402

Schiber A, Mihalev K, Berardini N, Mollov P, Carle R. Flavonol glycosides from distilled petals of *Rosa damascena* Mill. Z Naturforsch C J Biosc, 2005; 60:379–84; doi:10.1515/znc-2005-5-602

Singh A, Bajpai V, Kumar S, Sharma KR, Kumara B. Profiling of gallic and ellagic acid derivatives in different plant parts of *Terminalia arjuna* by HPLC-ESI-QTOF-MS/MS. Nat Prod Commun, 2016; 11:239–44.

Skehan P, Storeng R, Scudiero D, Monks A, McMahon I, Vistica D. New colorimetric cytotoxicity assay for anticancer drug screening. J Nat Cancer Inst, 1990; 82:1107–12; doi:10.1093/jnci/82.13.1107

Solimine J, Garo E, Wedler J, Rusanov K, Fertig O, Hamburger M, Atanassov I, Butterweck V. Tyrosinase inhibitory constituents from a polyphenol enriched fraction of rose oil distillation wastewater. Fitoterapia, 2016; 108:13–9; doi: 10.1016/j.fitote.2015.11.012

Stanila A, Diaconeasa Z, Roman I, Sima N, Maniutiu D, Roman A, Sima R. Extraction and characterization of phenolic compounds from rose Hip (*Rosa canina* L.) using liquid chromatography coupled with electrospray ionization- mass spectrometry. Not Bot Horti Agrobot Cluj Napoca, 2015; 43:349–54; doi: 10.15835/nbha43210028

Zhang Y, Shi P, Qu H, Cheng Y. Characterization of phenolic compounds in *Erigeron breviscapus* by liquid chromatography coupled to electrospray ionization mass spectrometry. Rapid Commun Mass Spectrom, 2007; 21:2971–84; doi:10.1002/rcm.3166

Zhu K-X, Lian C-X, Guo X-N, Peng W, Zhou H-M. Antioxidant activities and total phenolic contents of various extracts from defatted wheat germ. Food Chem, 2011; 126:1122–6; doi: 10.1016/j.foodchem.2010.11.144

How to cite this article:
Osman EEA, Bazaid SA, Abdel-Hameed ES. Chemo-profiling and bioactivities of Taif rose (*Rosa damascena* Mill.) industrial by-products after hydrodistillation. J Appl Pharm Sci, 2023; 13(10):119–131.